Int J Clin Exp Pathol 2024;17(10):329-345
www.ijcep.com /ISSN:1936-2625/IJCEP0158058

Original Article

Role of SLC31A1 in prognosis and immune infiltration in breast cancer: a novel insight

Zhen-Hua Luo[1], Bo Zhou[1], Jun-Yi Yu[1], He Li[1,3], Zan Li[1], Si-Qing Ma[2]

[1]Hunan Cancer Hospital and The Affiliated Cancer Hospital of Xiangya School of Medicine, Central South University, Changsha 410008, Hunan, The People's Republic of China; [2]Department of Pharmacy, Hunan Chest Hospital, Changsha 4100013, Hunan, The People's Republic of China; [3]Hunan Provincial Key Laboratory of The Research and Development of Novel Pharmaceutical Preparations, Changsha Medical University, Changsha 410219, Hunan, The People's Republic of China

Received May 26, 2024; Accepted October 4, 2024; Epub October 15, 2024; Published October 30, 2024

Abstract: Objective: Copper, an essential metal element for humans, plays vital functions in cancer prognosis and immunity. SLC31A1, a high-affinity copper transporter, helps regulate copper homeostasis and has been implicated in tumor prognosis through mechanisms such as drug resistance, autophagy, ferroptosis, and cuproptosis. However, the role of SLC31A1 in breast cancer (BRCA) and its association with tumor immune infiltration has not been fully elucidated. This study aimed to investigate the expression pattern of SLC31A1, its clinical significance, and its effect on tumor immune infiltration in BRCA. Methods: We comprehensively analyzed multiple datasets, including Gene Expression Profiling Interaction Analysis (GEPIA), Tumor Immune Estimation Resource (TIMER), UALCAN, and Kaplan-Meier (KM) plotter, to assess the expression of SLC31A1 and its prognostic value in BRCA. Additionally, TIMER and TISIDB were used to explore the correlation between SLC31A1 expression and the extent of tumor immune infiltration. Results: SLC31A1 was significantly upregulated in BRCA tissues compared to adjacent non-tumor tissues. Higher SLC31A1 expression levels were associated with poorer clinical outcome. Multivariate Cox regression analysis confirmed that SLC31A1 served as an independent prognostic indicator. Furthermore, SLC31A1 expression showed significant associations with various immunomodulators, chemokines, chemokine receptors, and tumor-infiltrating lymphocytes (TILs), including CD8+ T cells, CD4+ T cells, regulatory T cells (Tregs), follicular helper T cells (Tfh), neutrophils, M2 macrophages, tumor-associated macrophages (TAMs), and monocytes. These findings suggest that SLC31A1 may regulate macrophage polarization and T cell exhaustion in BRCA, contributing to immune evasion and poor prognosis. Conclusion: Our study underscores the importance of further research to explore the therapeutic potential of targeting SLC31A1 and to uncover its additional roles in BRCA beyond the known mechanisms of drug resistance, autophagy, ferroptosis, and cuproptosis.

Keywords: SLC31A1, breast cancer, prognosis, tumor-infiltrating immune cells

Introduction

Worldwide, breast cancer (BRCA) has surpassed lung cancer as the leading cause of cancer incidence and mortality among women, with an estimated 2.3 million new cases and 685,000 deaths annually [1]. In 2022, 287,850 new BRCA cases and 43,250 BRCA deaths are projected to occur in the United States. It has been the leading cause of cancer incidence in women, representing 31% of all cancer cases in women. More importantly, incidence from 2014 through 2018 continued a slow increase for BRCA (by 0.5% annually) [2]. BRCA is a heterogeneous tumor. The high degree of diversity within tumors as well as individuals determines the prognosis and therapeutic resistance of BRCA patients [3]. Thus, further identification of the heterogeneity of cancer cell populations and their microenvironment remains an urgent need.

As an essential metal element for humans, copper was recognized early as a cofactor for many biochemical enzymes [4]. Indeed, the traditional view of copper as solely an active site metabolic cofactor has been challenged by emerging evidence that copper can induce various forms

https://doi.org/10.62347/LOYI1808

of programmed cell death, including apoptosis, autophagy, ferroptosis and cuproptosis [5-7]. Interestingly, cancer cells have a higher demand for copper compared to normal cells, with elevated copper levels observed in various cancer types, including breast [8, 9], gastrointestinal [10-12], lung [13, 14], thyroid [15], oral [16], bladder [17] and prostate cancers [18]. Solute carrier family 31 member 1 (SLC31A1) is a high-affinity copper transporter that helps regulate copper homeostasis [19]. Copper influx enhances MEK1 phosphorylation of ERK1/2 through a Cu-MEK1 interaction, and reducing SLC31A1 levels inhibits BRAF(V600E)-driven signaling and tumorigenesis [20]. In pancreatic cancer, blockage of SLC31A1-dependent copper absorption increases pancreatic cancer cell autophagy to resist cell death [21]. Recently, it was suggested that copper is an essential regulator of the autophagic kinases ULK1/2. In lung cancer, genetic ablation of SLC31A1 decreases autophagy and proliferation to reduce tumorigenesis and sensitizes cancer cells to starvation [22]. SLC31A1 also affects ferroptosis and cuproptosis by altering intracellular Cu^+ levels [23, 24]. Its expression is linked to platinum resistance in various cancers [25-29]. A phase I clinical trial combining trientine (a copper chelator) with carboplatin has shown promising results [30].

Recent advances in cancer immunotherapy have proven a prospective prognostic role of differential immune infiltrates densities in cancer patients [31]. Distinct oncogenic effect of the copper-SLC31A1 axis was found to not only target oncoproteins including MEK, ULK, Memo, and PDK1 but also modulate the immune response through manipulating immune cells such as T cells, B cells, natural killer (NK) cells and macrophages [32]. It also revealed that SLC31A1 expression was strongly correlated with the expression of PD-L1 across many cancers and intra-tumoral copper modulates PD-L1 expression and influences tumor immune evasion [33]. However, the relation between SLC31A1 and tumor-infiltrating immune cells in BRCA remains unclear. In summary, as an essential copper mediator, SLC31A1 is considered to play an important role in immune infiltration and might function as a prognostic biomarker in BRCA.

In this study, we explored the RNA and protein expression levels of SLC31A1 in BRCA patients and investigated the correlation between SLC31A1 expression and patient prognosis. Our results uncovered an association of SLC31A1 with tumor-infiltrating immune cells and highlighted the potential utility of its novel prognostic role in BRCA.

Materials and methods

Gene expression analysis

The Gene Expression Profiling Interactive Analysis (GEPIA) online database (e (http://gepia.cancer-pku.cn/index.html)) was imported to analyze the SLC31A1 expression level in BRCA tissues and normal tissues [34]. The ROC curve (Receiver Operating Characteristic curve) and the expression of SLC31A1 in BRCA samples and adjacent normal tissue were assessed by utilizing Xiantao database (https://www.xiantao.love/). The immunohistochemistry image of SLC31A1 were found in the HPA database (https://www.proteinatlas.org/).

UALCAN analysis

UALCAN is a comprehensive, easily used, and interactive web resource for analyzing cancer OMICS data (http://ualcan.path.uab.edu/index.html) [35]. In this study, UALCAN database was performed to explore the expression profile of SLC31A1 based on clinicopathologic factors, including sample types, individual cancer stages, age, cancer subclasses, nodal metastasis status, and TP53 mutation status.

Kaplan-Meier plotter (breast cancer)

The Kaplan Meier plotter (http://kmplot.com/analysis/index) is capable to evaluate the influence of the expression of all genes (mRNA, miRNA and protein) on prognosis in more than 30,000 samples from 21 tumor types including breast, ovarian, lung and gastric cancer for the databases include GEO, TCGA and EGA [36]. In the study, the prognostic values of SLC31A1 expression in BRCA, including overall survival (OS), relapse-free survival (RFS), distant metastasis-free survival (DMFS) and post-progression survival (PPS) were assessed. The hazard ratio (HR) with 95% confidence intervals was also

estimated, as well as the log-rank *p*-value. Significance was defined as $P < 0.05$.

TIMER (Tumor Immune Estimation Resource) analysis

TIMER 2.0 database (http://timer.cistrome.org/) is a comprehensive resource for systematical resource analysis of the interaction of immune infiltrates and gene expression, mutation status, somatic CNV and clinical outcome across diverse cancer types [37]. In this study, we estimated the association between immune infiltrates and SLC31A1 expression in BRCA. Since tumor purity is negatively correlated with most immune cell types, tumor purity is adjusted as a major confounding factor in this analysis. Furthermore, the correlation between the SLC31A1 expression and gene markers of different tumor-infiltrating immune cells, including CD8+/CD4+ T cells, myeloid dendritic cell, B cells, monocytes, mast cell, macrophages, neutrophils, T cells, and related subtypes.

TISIDB

TISIDB (http://cis.hku.hk/TISIDB/index.php) is a repository portal with multiple heterogeneous data types for tumor and immune system interactions. This database devotes to elucidate the interplay of tumor and immune cells, which would assist both the prediction of immunotherapy responses and the development of novel immunotherapy targets [38]. In this research, TISIDB was utilized to estimate the association of SLC31A1 expression with tumor-infiltrating lymphocytes (TILs), immunostimulators, immunoinhibitors, chemokines, and receptors in BRCA.

Statistical analysis

The survival curves were calculated by the KM plot with long-rank test. Univariate and multivariate Cox regression were performed to identify the prognostic value of clinicopathologic characteristics on survival. The nomogram model was constructed to predict the 3, 5-year survival probability. The calibration curves were to evaluate the concordance of the observed and predicted rates of 3, 5-year OS [39]. Spearman correlation analysis was utilized to assess the association of SLC31A1 expression and immune infiltration levels and gene markers of TILs. All the analyses were performed with SPSS (version 25.0). $P < 0.05$ was defined as significant.

Results

SLC31A1 is aberrantly upregulated in breast cancer

As presented in **Figure 1A**, compared with non-neoplastic normal tissues, SLC31A1 expression levels were significantly higher in bladder urothelial carcinoma ($P < 0.05$), breast invasive carcinoma ($P < 0.01$), cervical squamous cell carcinoma and endocervical adenocarcinoma ($P < 0.05$), esophageal carcinoma ($P < 0.01$), glioblastoma ($P < 0.001$), head and neck squamous cell carcinoma ($P < 0.05$), prostate adenocarcinoma ($P < 0.01$), stomach adenocarcinoma ($P < 0.001$), and uterine corpus endometrial carcinoma ($P < 0.001$), but lower in Cholangiocarcinoma ($P < 0.001$), renal cell carcinoma ($P < 0.001$), hepatocellular carcinoma ($P < 0.001$), lung cancer ($P < 0.001$), prostatic adenocarcinoma ($P < 0.001$), and thyroid carcinoma ($P < 0.001$).

In breast cancer (BRCA), SLC31A1 expression was significantly elevated in tumor tissues compared to normal breast tissues (GEPIA, $P < 0.001$; **Figure 1B**), and was upregulated in tumor tissues compared to paired para-cancerous tissues (n=112; **Figure 1C**; $P < 0.001$). The AUC for SLC31A1 mRNA in BRCA was 0.801 (95% CI 0.774-0.829; **Figure 1D**). Protein expression analysis using the HPA dataset confirmed increased SLC31A1 levels in BRCA tissues (**Figure 1E**). These results suggest that SLC31A1 may serve as a diagnostic biomarker for BRCA.

Relationship of SLC31A1 expression with clinical pathology in BRCA

To clarify the relationship between SLC31A1 expression and several clinicopathologic parameters, analyses were performed on its association with sample types, individual cancer stages, patient age, breast cancer subclasses, nodal metastasis status and TP53 mutation status was analyzed (**Figure 2**; Table S1).

SLC31A1 expression was significantly higher in BRCA samples compared to normal tissues (**Figure 2A**, $P < 0.001$). No significant difference in SLC31A1 expression was observed

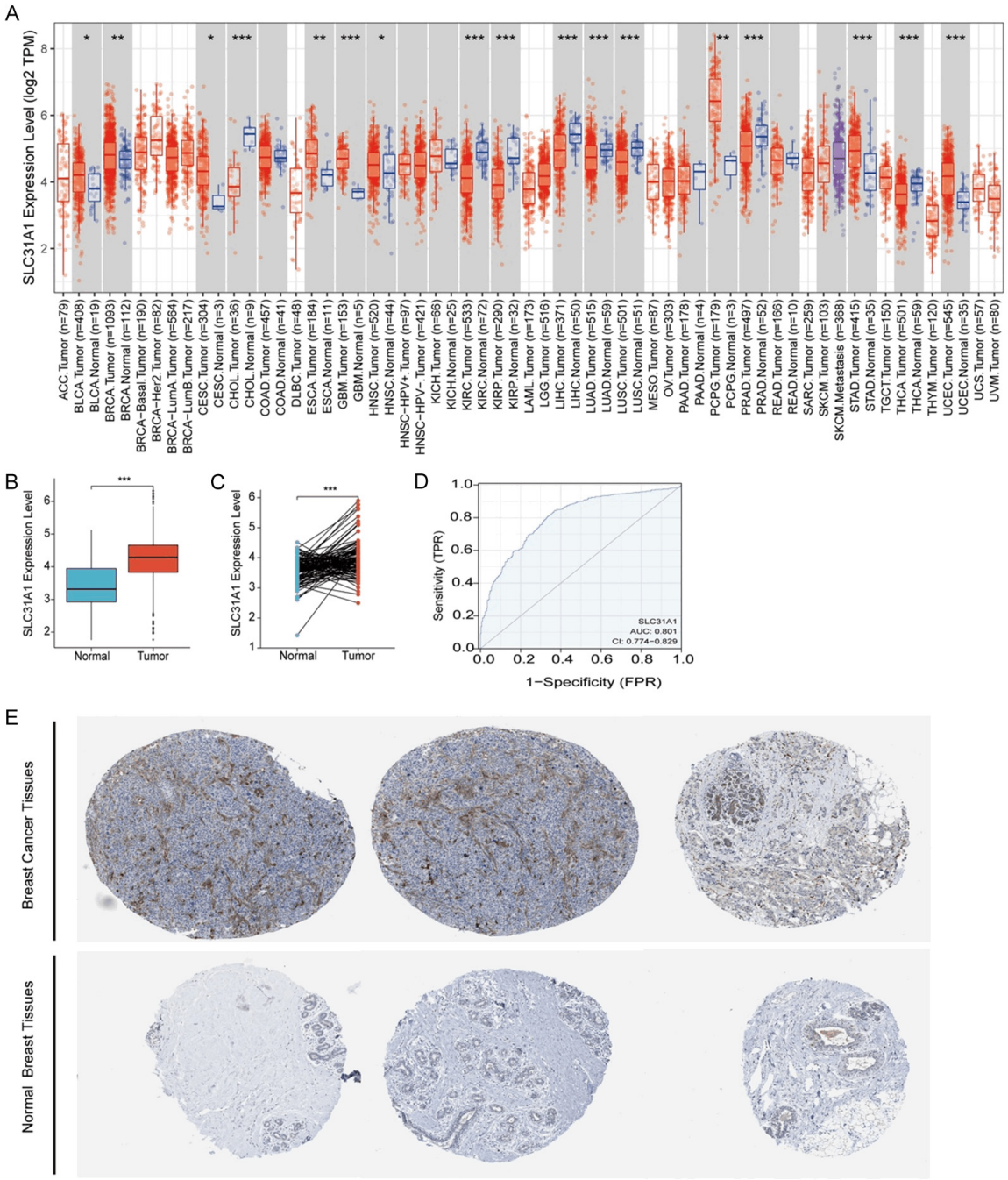

Figure 1. Expression pattern of SLC31A1 in breast cancer (BRCA). A. Differential expression of SLC31A1 in various cancers was analyzed by TIMER; B. Increased SLC31A1 in BRCA tissues compared with normal tissues in GEPIA; C. Increased SLC31A1 expression in BRCA compared with the matching normal tissue from Xiaotao dataset; D. The receiver-operating characteristic (ROC) curve analysis of SLC31A1 in BRCA patients; E. The expression of SLC31A1 protein in BRCA patients from HPA dataset (*P < 0.05, **P < 0.01, ***P < 0.001).

among BRCA stages (**Figure 2B**), though stage 4 patients were found to have higher expression levels than stage 2 patients (*P=0.00281*). Patients aged 21-40 years showed substantially lower SLC31A1 expression compared to those aged 41-60 years and 61-80 years (**Figure 2C**, *P < 0.001* for both). Higher SLC31A1 expression was noted in HER2-positive patients compared to luminal and triple-negative breast cancer patients (**Figure 2D**). No associa-

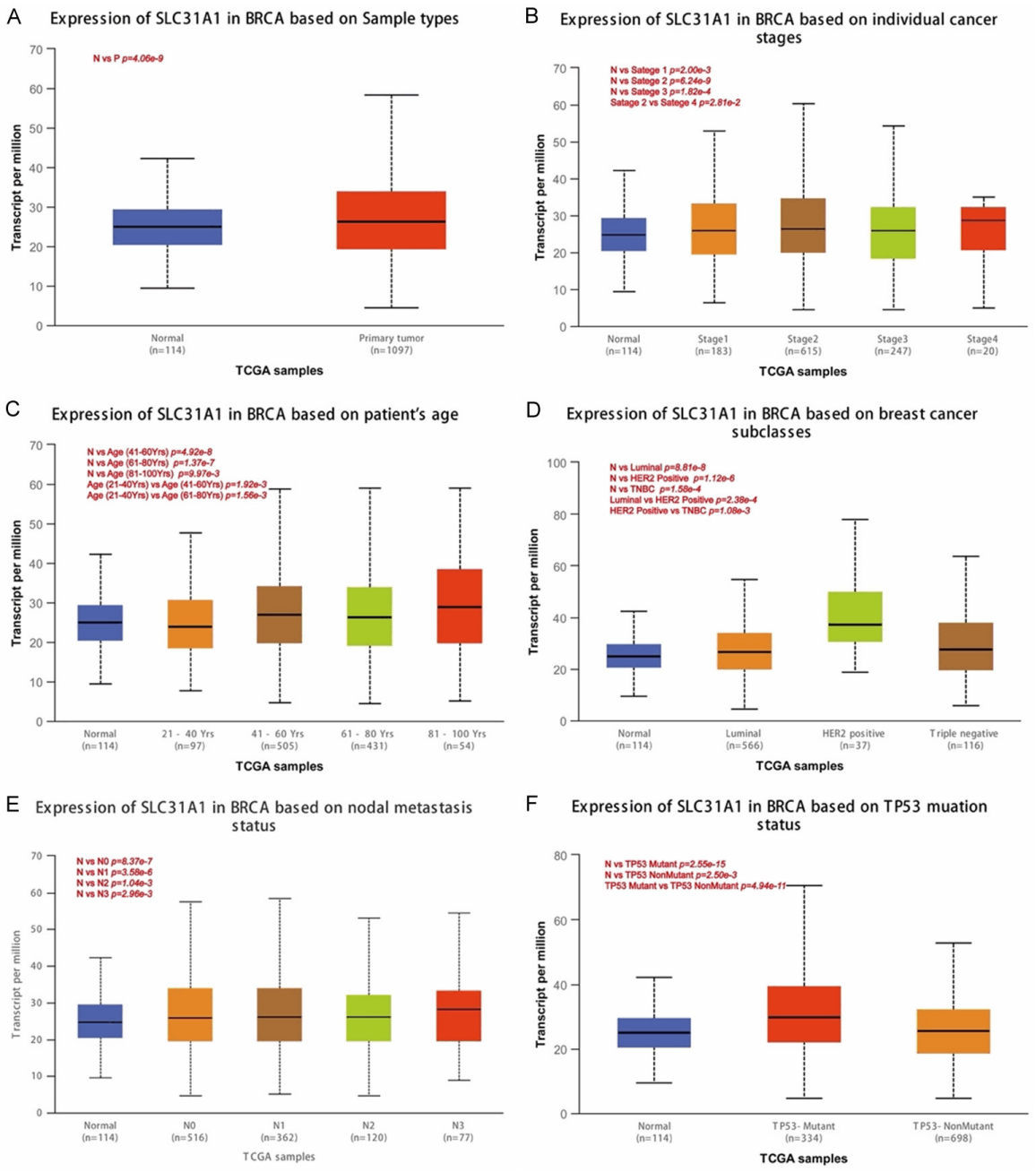

Figure 2. Correlation between SLC31A1 mRNA expression and clinicopathologic data of BRCA through the UALCAN database. A. Sample type; B. Individual cancer stage; C. Patients' age; D. Breast cancer subclasses; E. Nodal metastasis; F. TP53 mutation status.

tion was detected between SLC31A1 expression and lymph node metastasis (**Figure 2E**). Elevated SLC31A1 levels were found in BRCA patients with TP53 mutations compared to those with TP53 wildtype (**Figure 2F**, *P < 0.001*). Furthermore, SLC31A1 expression was associated with race (*P=0.004*), histological type (*P < 0.001*), ER status (*P < 0.001*), HER2 status (*P=0.026*), PAM50 (*P < 0.001*), and overall survival events (P=0.007; Table S1).

SLC31A1 is associated with poor prognosis and is an independent prognostic predictor in BRCA

A Kaplan-Meier plotter was used to assess the survival value of SLC31A1 in BRCA (**Figures 3**

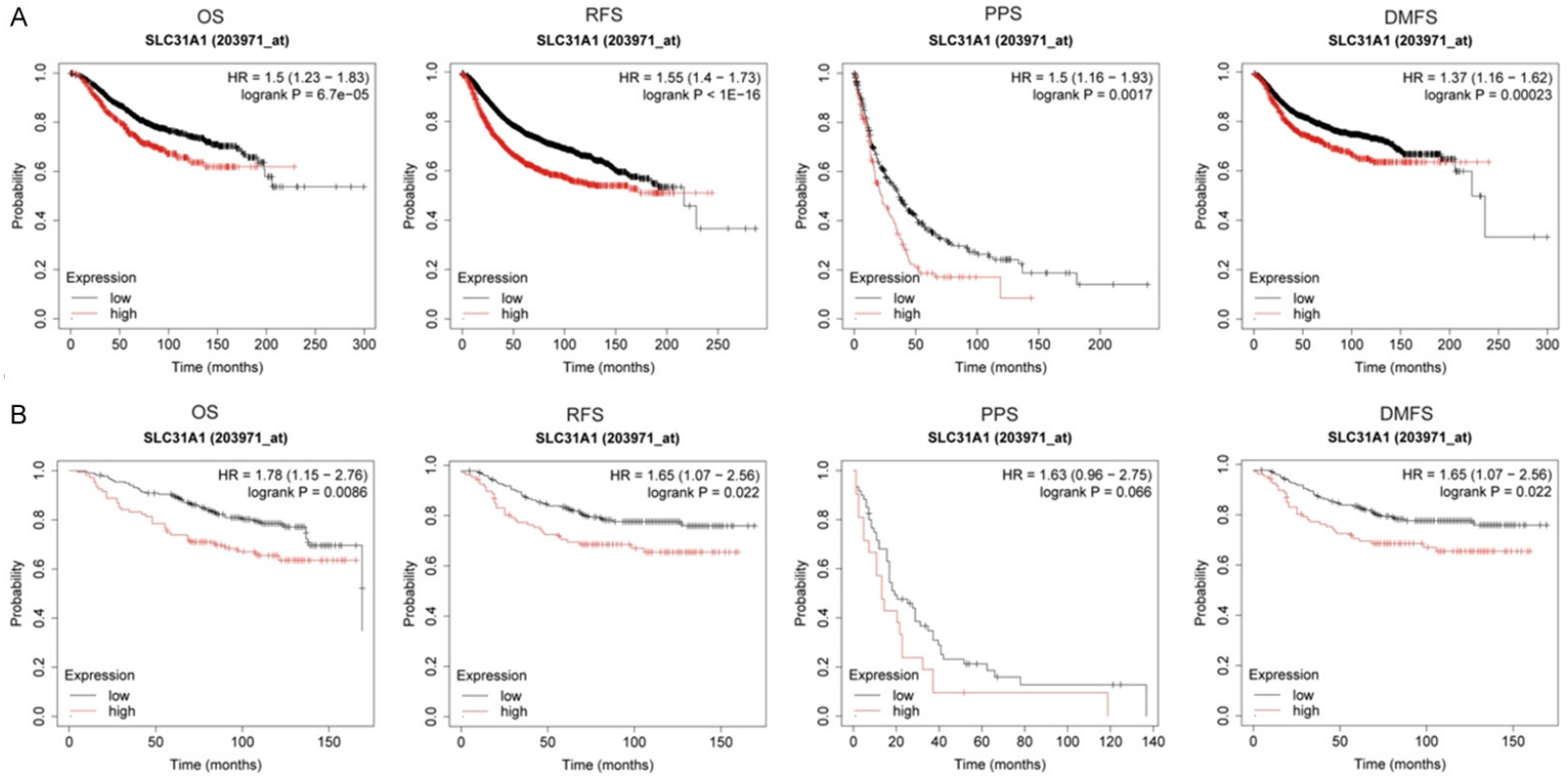

Figure 3. KM survival curve to show the association between SLC31A1 and clinical outcome in BRCA in KM Plotter dataset. A. Survival curves of OS, RFS, PPS and DMFS in all datasets cohort; B. Survival curves of OS, RFS, PPS and DMFS in GSE20685 cohort. OS: Overall survival; RFS: Relapse-free survival; PPS: Post-progression survival; DMFS: Distant metastasis-free survival.

Table 1. Association between clinicopathologic parameters and overall survival (OS) in BRCA by using Univariate and Multivariate Cox regression analysis

Characteristics	Total (N)	Univariate Cox regression analysis		Multivariate Cox regression analysis	
		HR (95% CI)	*P* value	HR (95% CI)	*P* value
Pathologic stage	1059				
Stage I	180	Reference			
Stage II	619	1.697 (0.985-2.922)	0.057	4.038 (0.777-20.972)	0.097
Stage III	242	2.962 (1.664-5.273)	< 0.001	1.598 (0.609-4.196)	0.146
Stage IV	18	11.607 (5.569-24.190)	< 0.001	13.088 (1.027-166.827)	0.048
N Stage	1063				
N0	514	Reference			
N1	357	1.956 (1.329-2.879)	< 0.001	0.862 (0.315-2.360)	0.772
N2	116	2.519 (1.482-4.281)	< 0.001	2.323 (0.400-13.486)	0.348
N3	76	4.188 (2.316-7.574)	< 0.001	4.334 (0.723-25.977)	0.108
M stage	922				
M0	902	Reference			
M1	20	4.254 (2.468-7.334)	< 0.001	1.863 (0.733-4.733)	0.191
T stage	1079				
T1	276	Reference			
T2	629	1.334 (0.889-2.002)	0.164	0.639 (0.207-1.969)	0.435
T3	139	1.572 (0.933-2.649)	0.089	1.216 (0.327-4.520)	0.770
T4	35	3.755 (1.957-7.205)	< 0.001	2.797 (0.531-14.733)	0.225
Age	1082				
≥ 60 y	601	Reference			
< 60 y	481	2.020 (1.465-2.784)	< 0.001	2.766 (1.309-5.845)	0.008
Radiation Therapy	986				
No	434	Reference			
Yes	552	0.576 (0.394-0.841)	0.004	0.480 (0.234-0.984)	0.045
Menopause status	931				
Pre	229	Reference			
Post	702	2.165 (1.302-3.600)	0.003	3.896 (1.218-12.468)	0.022
SLC31A1 (Median)	1082				
Low expression	540	Reference			
High expression	542	1.586 (1.146-2.196)	0.005	1.345 (1.068-2.651)	0.042

and S2). Increased expression of SLC31A1 mRNA was significantly associated with reduced OS (HR: 1.50; 95% CI: 1.23-1.83; *P=6.7e-05*), RFS (HR: 1.55; 95% CI: 1.40-1.73; *P < 1e-16*), PPS (HR: 1.50; 95% CI: 1.16-1.93; *P=0.0017*) and DMFS (HR: 1.37; 95% CI: 1.16-1.62; *P=0.00023*) in all available datasets (**Figure 3A**). Analysis of GSE20685 (N=327) showed similar results (**Figure 3B**, N=327): higher SLC31A1 mRNA expression correlated with worse OS (HR: 1.78; 95% CI: 1.15-2.76; *P=0.0086*), RFS (HR: 1.65; 95% CI: 1.07-2.56; *P=0.022*) and DMFS (HR: 1.65; 95% CI: 1.07-2.56; *P=0.022*). PPS showed a shorter tendency but was not significantly different (HR: 1.63; 95% CI: 0.96-2.75; *P=0.066*).

Based on the above findings, we further performed univariate and multivariate Cox regression to identify the prognostic risk factors. As presented in **Table 1**, Stage III (HR: 2.962; 95% CI: 1.664-5.273; *P < 0.001*), Stage IV (HR: 11.607; 95% CI: 5.569-24.190; *P < 0.001*); N1 (HR: 1.956; 95% CI: 1.329-2.879; *P < 0.001*), N2 (HR: 2.519; 95% CI: 1.482-4.281; *P < 0.001*), N3 (HR: 4.188; 95% CI: 2.316-7.574; *P < 0.001*), M1 stage (HR: 4.254; 95% CI: 2.468-7.334; *P < 0.001*), T4 stage (HR: 3.755; 95% CI: 1.957-7.205; *P < 0.001*), younger age

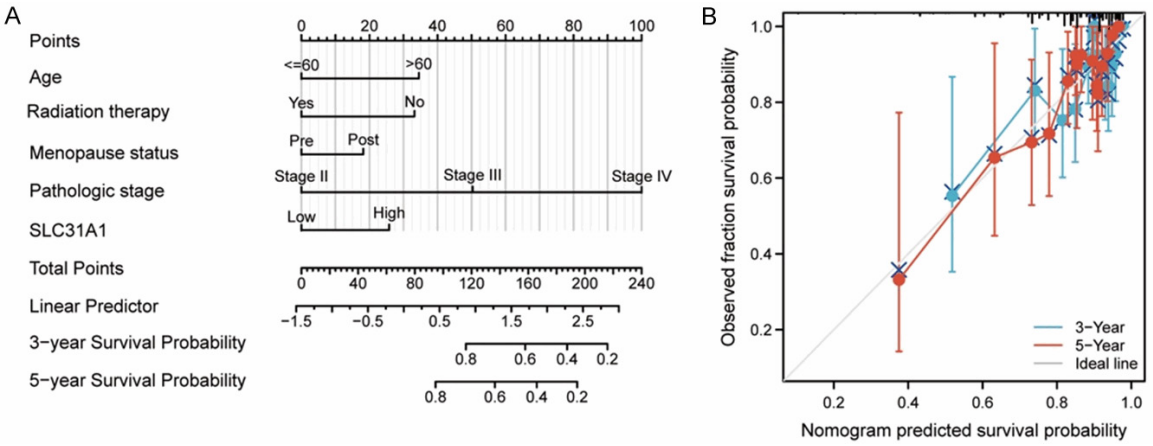

Figure 4. Construction of nomogram based on SLC31A1 and clinical parameters. A. Construction of nomogram based on SLC31A1 and clinical data; B. Calibration plots of the nomogram for predicting the probability of OS at 3, and 5-years.

(HR: 2.020; 95% CI: 1.465-2.784; *P < 0.001*), post menopausal status(HR: 2.165; 95% CI: 1.302-3.600; *P=0.003*) and high expression of SLC31A1 (HR: 1.586; 95% CI: 1.146-2.196; *P=0.003*) were associated with the worse OS by performing univariate Cox regression analysis. On the contrary, radiation therapy indicated better OS of patients (HR: 0.576; 95% CI: 0.394-0.841; *P=0.004*).

Multivariate Cox regression analysis results uncovered that Stage IV (HR: 13.088; 95% CI: 1.027-166.827; *P=0.048*), age (HR: 2.766; 95% CI: 1.309-5.845; *P=0.008*), radiation therapy (HR: 0.480; 95% CI: 0.234-0.984; *P=0.045*), menopause status (HR: 3.896; 95% CI: 1.218-12.468; *P=0.022*) and SLC31A1 mRNA expression (HR: 1.345; 95% CI: 1.068-2.651; *P=0.042*) were all independent risk factor of OS in BRCA. Furthermore, a nomogram based on the risk predictors was constructed (**Figure 4A**). Calibration plots showed that the observed vs. predicted rates of 3- and 5-year OS showed perfect concordance (**Figure 4B**).

Correlation between immune infiltration and SLC31A1 expression in BRCA

TISIDB and TIMER datasets were utilized to evaluate the correlation between immune infiltration and SLC31A1 expression. In TISIDB, SLC31A1 expression were positively correlated with the abundance of the several TILs (**Figure 5A**), including Central memory CD8 T cell (Tcm_CD8, rho=0.107, *P=0.000382*), activated CD4 T cell (Act_CD4, rho=0.257, *P=5.86e-18*), effector memory CD4 T cell (Tem_CD4, rho=0.166, *P=3.03e-8*), T follicular helper cell (Tfh, rho=0.101, *P=0.000848*), Type 2 T helper cell (Th2, rho=0.258, *P=4.10e-18*), regulatory T cell (Treg, rho=0.097, *P=0.00129*), activated dendritic cell (Act_DC, rho=0.198, *P=4.05e-11*), and myeloid-derived suppressor cell (MDSC, rho=0.064, *P=0.0328*). Correlations with 22 immune cells are shown in **Figure 5B**, and the infiltrates estimation value with SLC31A1 expression is shown in **Figures 5C** and S1.

In the TIMER platform, SLC31A1 expression was positively correlated with infiltration levels of CD8+ T cell (Rho=0.263, *P=3.06e-17*), CD4+ T Cell (Rho=0.257, *P=2.07e-16*), myeloid dendritic cell (Rho=0.111, *P=4.69e-4*), Macrophage (Rho=0.247, *P=2.88e-15*), mast cell (Rho=0.183, *P=5.65e-9*), monocyte (Rho=0.154, *P=1.02e-6*), neutrophil (Rho=0.327, *P=3.99e-26*), Tegs (Rho=0.307, *P=4.33e-23*), Tfh (Rho=0.152, *P=3.45e-3*) and B cell (Rho=0.118, *P=1.98e-4*). Moreover, we found that SLC31A1 was significantly associated with the majority of markers sets of M2 macrophages, TAM, neutrophils, Tregs, several functional T cells and T cell exhaustion in TIMER dataset (**Table 2**). We further validated the connection of SLC31A1 expression with the aforementioned markers of M2 macrophages, TAM, neutrophils, Tregs, Th1, Th2, Th17 and T cell exhaustion in the GEPIA dataset (Table S3). Similarly, SLC31A1 was assessed to be correlated with the gene markers of M2 macrophages, TAM, Tregs, Th1, Th2

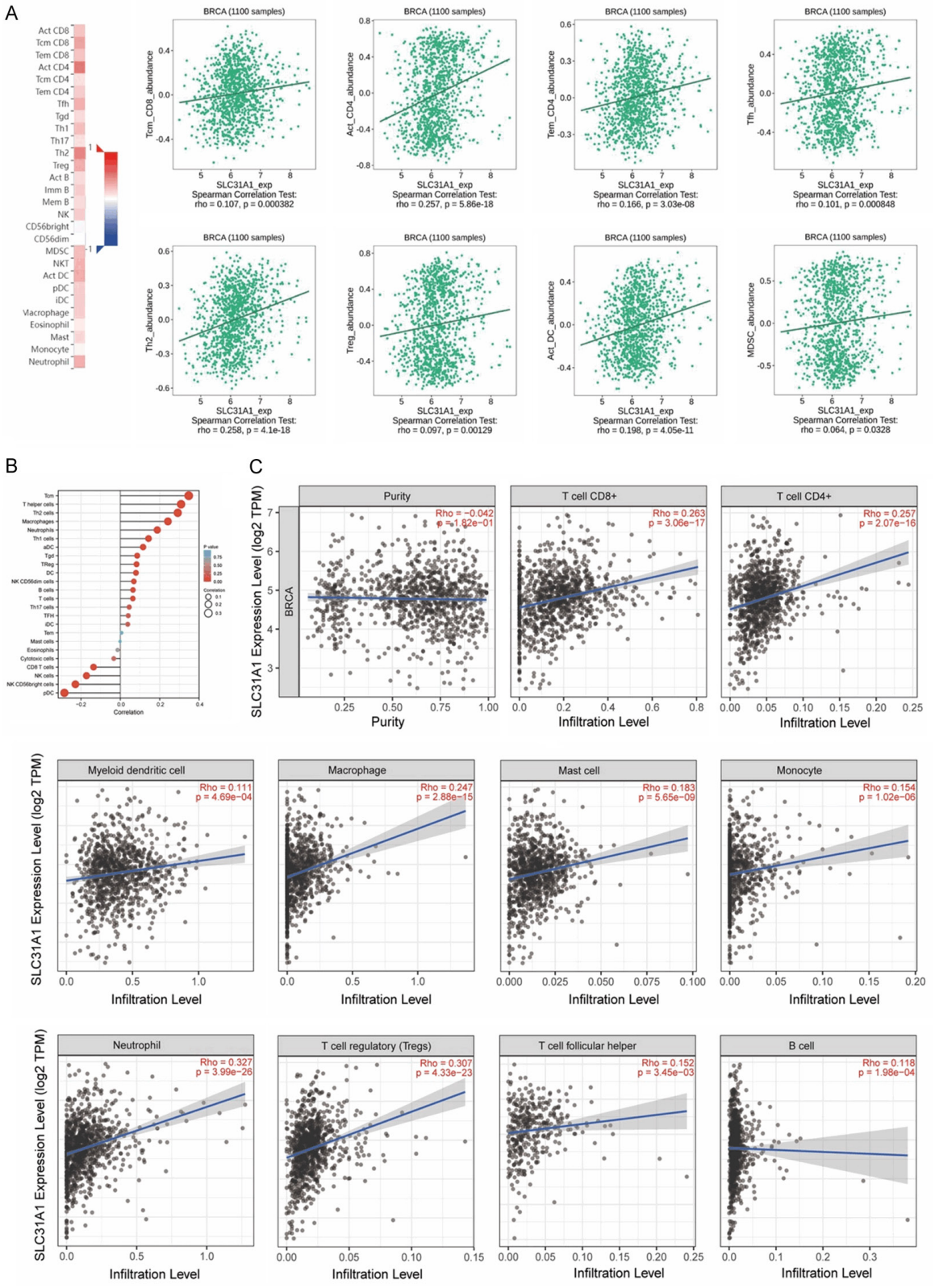

Figure 5. Correlation of SLC31A1 expression with immune infiltration in BRCA. A. Correlation between the expression of SLC31A1 and the abundance of TILs in BRCA available at TISIDB database; B. Lollipop figure to show the correlation between SLC31A1 and infiltration degree in Xiantao dataset; C. Correlation of ITGAL expression with infiltration levels of CD8+ T cells, CD4+ T cells, Myeloid dendritic cells, macrophages, mast cells, monocytes, neutrophils, Treg cells, T cell follicular helper cells (Tfh) and B cells in BRCA available at TIMER2.0 database.

Table 2. Correlation between SLC31A1 and gene markers of immune cells in TIMER 2.0 platform

Description	Gene markers	BRCA			
		None Adjustment		Purity Adjustment	
		Rho	*p* value	Rho	*p* value
CD8+ T cell	CD8A	0.113	*< 0.0001*	0.108	*< 0.0001*
	CD8B	0.038	0.213	0.033	0.102
T cell (general)	CD18	0.133	*< 0.0001*	0.132	*< 0.0001*
	CD3D	0.045	0.133	0.033	0.302
	CD3E	0.08	*< 0.001*	0.073	*< 0.01*
CD4+ T cell	CD4	0.203	*< 0.0001*	0.208	*< 0.0001*
	CD127	0.311	*< 0.0001*	0.341	*< 0.0001*
MDC	LYZ	0.275	*< 0.0001*	0.298	*< 0.0001*
	IRF7	-0.236	*< 0.0001*	-0.247	*< 0.0001*
TAM	CCL18	0.174	*< 0.001*	0.196	*< 0.001*
	CD163	0.305	*< 0.0001*	0.310	*< 0.0001*
	IL10	0.238	*< 0.0001*	0.24	*< 0.0001*
	CD206	0.269	*< 0.0001*	0.282	*< 0.0001*
M1 macrophage	NOS2	0.097	*< 0.001*	0.094	*< 0.001*
	IRF5	0.027	0.374	0.013	0.678
M2 macrophage	VSIG4	0.201	*< 0.0001*	0.195	*< 0.0001*
	MS4A4A	0.257	*< 0.0001*	0.264	*< 0.0001*
	CLEC7A	0.333	*< 0.0001*	0.337	*< 0.0001*
	CD273	0.306	*< 0.0001*	0.330	*< 0.0001*
Mast cell	CST3	-0.350	*< 0.0001*	-0.361	*< 0.0001*
	CPA3	0.104	*< 0.0001*	0.101	*< 0.001*
Monocyte	CD86	0.244	*< 0.0001*	0.247	*< 0.0001*
	CD115	0.173	*< 0.0001*	0.163	*< 0.0001*
Neutrophils	CD66b	0.011	0.708	0.015	0.835
	CD11b	0.252	*< 0.0001*	0.237	*< 0.0001*
	CCR7	0.078	*< 0.001*	0.077	*< 0.001*
	FCGR3B	0.199	*< 0.0001*	0.208	*< 0.0001*
	CSF3R	0.026	0.396	0.008	0.886
Tregs	FOXP3	0.217	*< 0.0001*	0.226	*< 0.0001*
	CCR8	0.332	*< 0.0001*	0.334	*< 0.0001*
	STAT5B	0.102	*< 0.0001*	0.088	*< 0.001*
	TGFB1	-0.018	0.759	-0.048	0.234
	CCR10	-0.16	*< 0.0001*	-0.175	*< 0.0001*
	CD25	0.277	*< 0.0001*	0.286	*< 0.0001*
	CD52	0.035	0.363	0.015	0.630
	CMTM7	-0.02	0.516	-0.035	0.384
Tfh	BCL6	0.131	*< 0.0001*	0.146	*< 0.0001*
	IL21	0	0.998	-0.012	0.711
	BATF	-0.238	*< 0.0001*	-0.251	*< 0.0001*
	CXCR5	0.047	0.117	0.035	0.276
Th1	TBX21	0.089	*< 0.001*	0.084	*< 0.001*
	STAT4	0.152	*< 0.0001*	0.150	*< 0.0001*
	STAT1	0.359	*< 0.0001*	0.351	*< 0.0001*
	IFNG	0.159	*< 0.0001*	0.162	*< 0.0001*
	TNF	0.095	*< 0.001*	0.094	*< 0.001*

Th2	GATA3	-0.113	*< 0.0001*	-0.131	*< 0.0001*
	STAT6	0.064	*< 0.01*	0.063	*< 0.01*
	STAT5A	0.03	0.314	0.009	0.773
	IL13	0.09	*< 0.001*	0.087	*< 0.001*
Th17	STAT3	0.367	*< 0.0001*	0.349	*< 0.0001*
	IL17A	0.099	*< 0.001*	0.097	*< 0.001*
B cell	CD19	-0.007	0.818	-0.031	0.322
	CD79A	0.014	0.632	0	1.00
	CD79B	-0.063	*< 0.01*	-0.103	*< 0.001*
	MS4A1	0.055	0.067	0.044	0.167
T cell exhaustion	PDCD1	0.02	0.502	0.003	0.918
	PDCD1LG2	0.306	*< 0.0001*	0.330	*< 0.0001*
	CTLA4	0.142	*< 0.0001*	0.140	*< 0.0001*
	LAG3	0.032	0.295	0.025	0.424
	HAVCR2	0.265	*< 0.0001*	0.265	*< 0.0001*
	GZMB	0.099	*< 0.0001*	0.094	*< 0.001*

Note: See Table S2 for exact *p*-values. MDC: Myeloid dendritic cells; TAM: Tumor-associated macrophages; Tregs: Regulatory T cell; Tfh: Follicular helper T cell; BRCA: Breast cancer.

and T cell exhaustion. Hence, SLC31A1 may regulate macrophage polarization and T cell exhaustion in BRCA.

SLC31A1 expression is associated with immunomodulators and chemokines in BRCA

Immunomodulators and chemokines play critical roles in the function of immune system. Therefore, the association between SLC31A1 expression and immunomodulators and chemokines was investigated. The results indicated that SLC31A1 was positively connected with various immunoinhibitors (**Figure 6A**), such as CD274 (Rho=0.281, *P=2.98e-21*), HAVCR2 (Rho=0.135, *P=7.68e-6*), IL10 (Rho=0.127, *P=2.49e-6*), IL10RB (Rho=0.142, *P=2.18e-6*), PCD1LG2 (Rho=0.177, *P=3.84e-9*), TGFBR1 (Rho=0.428, *P < 2.2e-16*), and negatively correlated with immunostimulators (**Figure 6B**), including C10orf54 (Rho=-0.133, *P=9.24e-6*), TNFRSF4 (Rho=-0.198, *P=3.47e-11*), TNFRSF13B (Rho=-0.133, *P=9.24e-6*), TNFRSF14 (Rho=-0.401, *P < 2.2e-16*), TNFRSF18 (Rho=-0.286, *P=3.6e-22*) and TNFRSF25 (Rho=-0.272, *P=5.1e-20*).

Additionally, SLC31A1 was positively linked with various chemokines, including CCL7 (Rho=0.174, *P=6.84e-9*), CCL8 (Rho=0.144, *P=1.66e-6*), CCL13 (Rho=0.107, *P=4.01e-4*), CCL18 (Rho=0.160, *P=9.34e-8*), CCL20 (Rho=0.130, *P=1.53e-5*), CXCL8 (Rho=0.187, *P=4.08e-10*), CXCL9 (Rho=0.141, *P=2.55e-6*), CXCL10 (Rho=0.181, *P=1.44e-9*), CXCL11 (Rho=0.172, *P=1.02e-8*) and CXCL17 (Rho=0.164, *P=5.01e-8*) (**Figure 7A**). Correlations with chemokine receptors were also found (**Figure 7B**), such as CCR1, CCR4, CCR5, and CCR8. These results suggest that SLC31A1 may participate in immune function regulation, contributing to tumor immune evasion.

Discussion

Breast cancer (BRCA) is the most prevalent cancer in women and the leading cause of cancer death, with about a half-million deaths annually despite advanced radiotherapy and chemotherapy treatments [40]. In this study, we comprehensively investigated the prognostic value of SLC31A1 in BRCA. Our results suggested that SLC31A1 was highly expressed in BRCA tissues compared with the adjacent normal tissue. High expression of SLC31A1 indicated poor survival outcomes. Moreover, our data demonstrated that SLC31A1 expression was significantly associated with immune infiltration degree, immunomodulators, chemokines, and receptors in BRCA. Findings suggest that SLC31A1 might function as a prognostic biomarker linked with immune infiltration in BRCA.

Evidence is showing that copper is not only an active site metabolic cofactor but also a dynam-

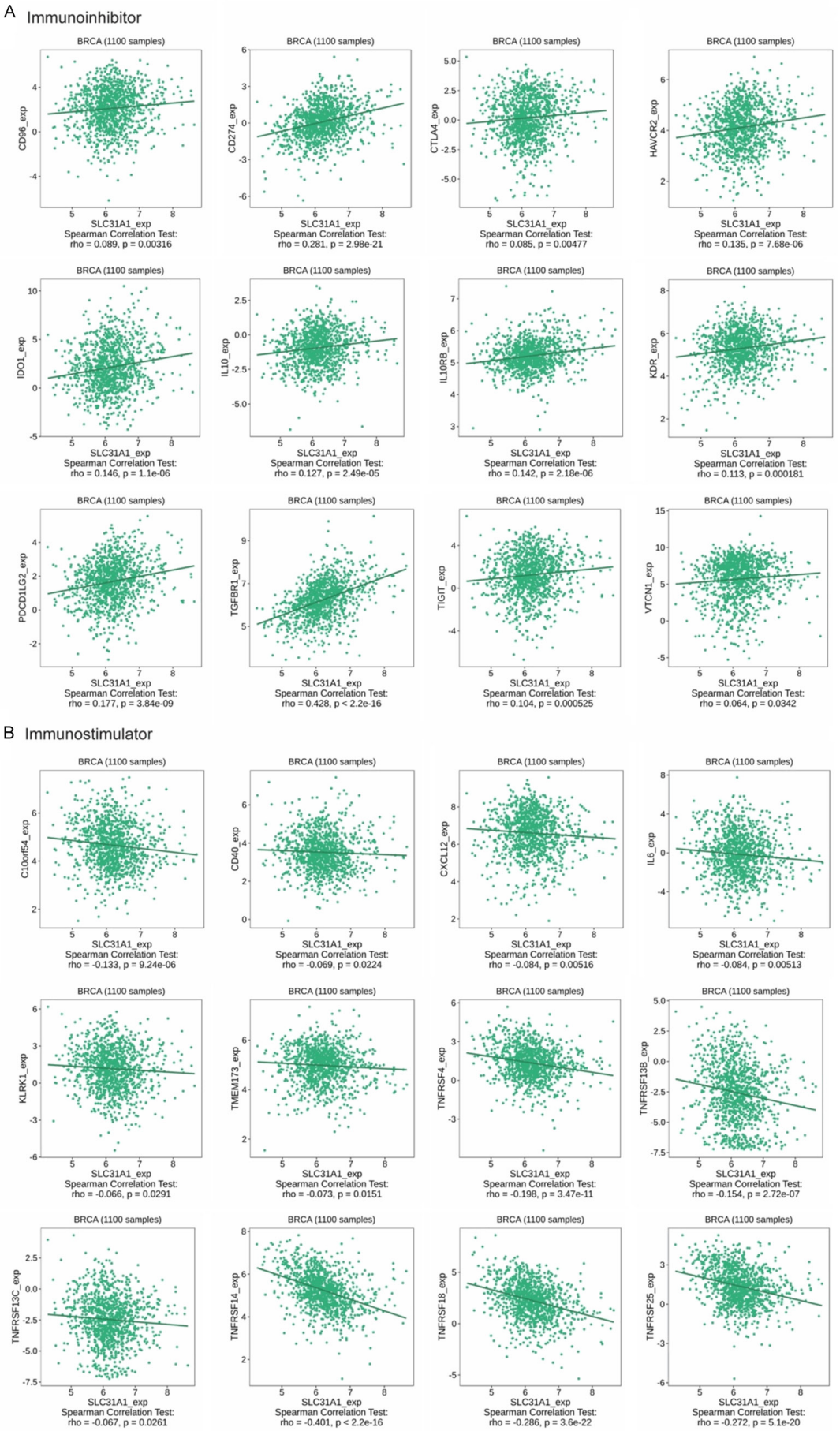
A Immunoinhibitor
BRCA (1100 samples)
CD96_exp
SLC31A1_exp
Spearman Correlation Test:
rho = 0.089, p = 0.00316
BRCA (1100 samples)
CD274_exp
SLC31A1_exp
Spearman Correlation Test:
rho = 0.281, p = 2.98e-21
BRCA (1100 samples)
CTLA4_exp
SLC31A1_exp
Spearman Correlation Test:
rho = 0.085, p = 0.00477
BRCA (1100 samples)
HAVCR2_exp
SLC31A1_exp
Spearman Correlation Test:
rho = 0.135, p = 7.68e-06
BRCA (1100 samples)
IDO1_exp
SLC31A1_exp
Spearman Correlation Test:
rho = 0.146, p = 1.1e-06
BRCA (1100 samples)
IL10_exp
SLC31A1_exp
Spearman Correlation Test:
rho = 0.127, p = 2.49e-05
BRCA (1100 samples)
IL10RB_exp
SLC31A1_exp
Spearman Correlation Test:
rho = 0.142, p = 2.18e-06
BRCA (1100 samples)
KDR_exp
SLC31A1_exp
Spearman Correlation Test:
rho = 0.113, p = 0.000181
BRCA (1100 samples)
PDCD1LG2_exp
SLC31A1_exp
Spearman Correlation Test:
rho = 0.177, p = 3.84e-09
BRCA (1100 samples)
TGFBR1_exp
SLC31A1_exp
Spearman Correlation Test:
rho = 0.428, p < 2.2e-16
BRCA (1100 samples)
TIGIT_exp
SLC31A1_exp
Spearman Correlation Test:
rho = 0.104, p = 0.000525
BRCA (1100 samples)
VTCN1_exp
SLC31A1_exp
Spearman Correlation Test:
rho = 0.064, p = 0.0342
B Immunostimulator
BRCA (1100 samples)
C10orf54_exp
SLC31A1_exp
Spearman Correlation Test:
rho = -0.133, p = 9.24e-06
BRCA (1100 samples)
CD40_exp
SLC31A1_exp
Spearman Correlation Test:
rho = -0.069, p = 0.0224
BRCA (1100 samples)
CXCL12_exp
SLC31A1_exp
Spearman Correlation Test:
rho = -0.084, p = 0.00516
BRCA (1100 samples)
IL6_exp
SLC31A1_exp
Spearman Correlation Test:
rho = -0.084, p = 0.00513
BRCA (1100 samples)
KLRK1_exp
SLC31A1_exp
Spearman Correlation Test:
rho = -0.066, p = 0.0291
BRCA (1100 samples)
TMEM173_exp
SLC31A1_exp
Spearman Correlation Test:
rho = -0.073, p = 0.0151
BRCA (1100 samples)
TNFRSF4_exp
SLC31A1_exp
Spearman Correlation Test:
rho = -0.198, p = 3.47e-11
BRCA (1100 samples)
TNFRSF13B_exp
SLC31A1_exp
Spearman Correlation Test:
rho = -0.154, p = 2.72e-07
BRCA (1100 samples)
TNFRSF13C_exp
SLC31A1_exp
Spearman Correlation Test:
rho = -0.067, p = 0.0261
BRCA (1100 samples)
TNFRSF14_exp
SLC31A1_exp
Spearman Correlation Test:
rho = -0.401, p < 2.2e-16
BRCA (1100 samples)
TNFRSF18_exp
SLC31A1_exp
Spearman Correlation Test:
rho = -0.286, p = 3.6e-22
BRCA (1100 samples)
TNFRSF25_exp
SLC31A1_exp
Spearman Correlation Test:
rho = -0.272, p = 5.1e-20

Figure 6. Correlation between SLC31A1 expression and immunomodulators in BRCA. A. Correlation between SLC31A1 expression and immunoinhibitors in BRCA available at TISIDB database. B. Correlation between SLC31A1 expression and immunostimulators in BRCA available at TISIDB database.

ic signaling metal and metalloallosteric regulator [41]. Due to its induction in multiple forms of programmed cell death, including apoptosis, autophagy, ferroptosis and cuproptosis, the intracellular copper level has attracted tremendous spotlight in the field of tumor treatment [42]. There is no doubt that SLC31A1, as an important copper importer, plays an important role in tumor progression. However, the possible function of SLC31A1 in regulating tumor immunity and its prognostic value in BRCA are still unclear.

In this present study, we comprehensively evaluated the clinical significance of SLC31A1 in BRCA using various databases. First, we revealed that SLC31A1 mRNA was aberrantly upregulated in BRCA tissues, compared with paracancerous normal tissues. The protein expression of SLC31A1 was also increased in BRCA samples, which was consistent with the mRNA expression pattern. These results suggested that SLC31A1 might be a diagnostic indicator in BRCA. To investigate the prognostic value of SLC31A1 in BRCA. The association between clinical feathers and SLC31A1 expression was researched. Moreover, KM Plotter was performed to explore the influence of SLC31A1 expression on OS, RFS, PPS and DMFS. The results suggested that higher expression of SLC31A1 indicated worse clinical outcome. By performing univariate and multivariate Cox regression analysis, SLC31A1 expressions were still related to OS, meaning that SLC31A1 was an independent prognostic factor. Besides, a high-performance nomogram, including SLC31A1 expression was constructed. All these data proved that SLC31A1 could function as a prognostic marker in BRCA.

Although BRCA is not considered a highly immunogenic tumor type, evidence is suggesting that TILs have may be a clinically relevant and highly reproducible biomarker capable of affecting BRCA prognosis [43, 44]. Intra-tumoral copper modulates PD-L1 expression and influences tumor immune evasion [33]. Recently, copper level was found to modulate the immune response through manipulating immune cells such as T cells, B cells, natural killer (NK) cells and macrophages [45]. However, the effect of SLC31A1 on tumor infiltration in BRCA was unknown. In the present study, we firstly identified that SLC31A1 was associated with immune infiltration in BRCA. Our study proved that SLC31A1 had a significant correlation with different TILs, including CD8+ T cell, CD4+ T cell, Treg cell, Tfh cell, neutrophils, M2 macrophages, TAM and monocytes.

Additionally, our data revealed an association between SLC31A1 and gene markers of various types of immune cells. As is known to us, TAMs are the most abundant infiltrating immune cells [46, 47]. Due to their plastic nature, TAMs may polarize into two forms, including M1 and M2 macrophages. In general, TAMs exhibit a M2-like phenotype, with high expression of CD163, CD206 and immunosuppressive factor IL10 to support immune escape and angiogenesis invasion and metastasis of cancer cells and remodeling of the extracellular matrix [48-50]. Our data showed that SLC31A1 had a strong association with gene markers of TAM and M2 macrophages, including CD163, CD273 and CLEC7A, while the correlation between SLC31A1 and M1 macrophages is very weak. All these results indicated that SLC31A1 may regulate macrophage polarization.

Although BRCA patients do not respond to immunotherapy and lung cancer and melanoma, a subset of BRCA, especially triple-negative breast cancer (TNBC), can benefit from the treatment of immune checkpoint inhibitors (ICIs). At present, atezolizumab in combination with the chemotherapeutic agent nab-paclitaxel has been approved to treat PD-L1-positive unresectable, locally advanced, or metastatic TNBC [51, 52]. Our results demonstrated that SLC31A1 expression was connected with Tregs marker (FOXP3, CCR8) and T cell exhaustion markers (PD-L2, CTLA4, HAVCR2), indicating that SLC31A1 may serve as a biomarker to screen BRCA patients with a robust response to the anti-CTLA-4 antibody Yervoy (ipilimumab). SLC31A1 was not only correlated with CTLA4 but also significantly correlated with several chemokines and chemokine receptors. Studies have proven that chemokines and che-

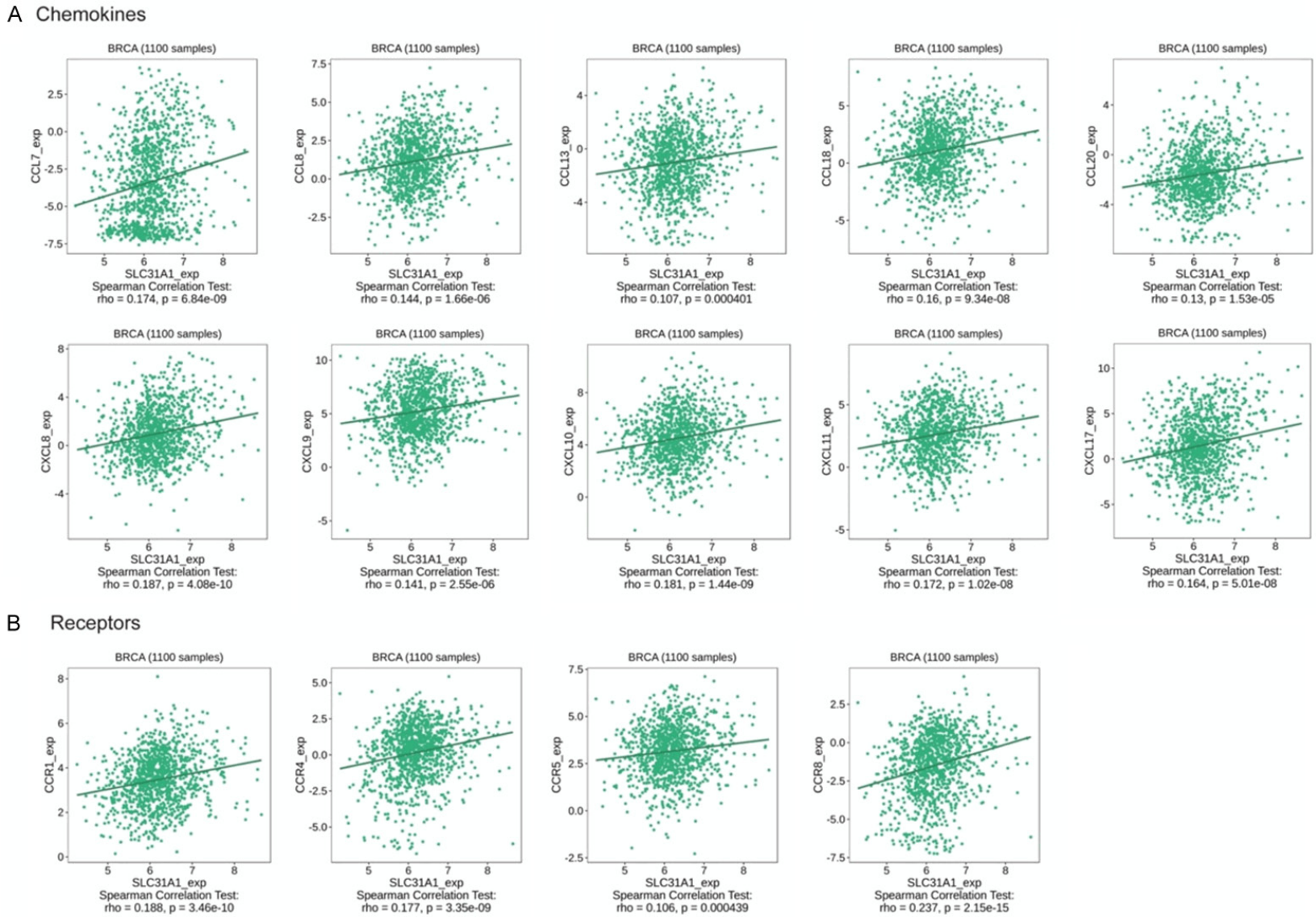

Figure 7. Correlation between the expression of SLC31A1 and chemokines in BRCA. A. Correlation between SLC31A1 expression and chemokines in BRCA available in the TISIDB database. B. Correlation between SLC31A1 expression and chemokine receptors in BRCA available in the TISIDB database.

mokine receptors participate in immune regulation, tumor growth, angiogenesis, metastases, and drug resistance in BRCA [53]. In conclusion, SLC31A1 may play vital functions in tumor immune infiltration in BRCA and the mechanisms of SLC31A1 in regulating tumor microenvironment in BRCA are worth investigating.

There are some limitations to our study. Firstly, most data are based on the Online platform, which is prone to be affected by a data update. Also, the prognostic value of SLC31A1 was not validated by BRCA samples and the molecular mechanism of SLC31A1 in BRCA was not explored *in vivo* and *in vitro* experiments.

Conclusions

SLC31A1 was found to be significantly upregulated in BRCA and linked to worse clinical outcome, suggesting its potential as an independent prognostic marker. It was associated with various immune cell types, including CD8+ T cells, CD4+ T cells, T follicular helper cells, regulatory T cells, and tumor-associated macrophages, indicating its role in immune regulation in BRCA. Further research is needed to explore SLC31A1's therapeutic potential and its broader impact in BRCA beyond drug resistance, autophagy, ferroptosis, and cuproptosis.

Acknowledgements

We wish to thank all the data of all the websites involved. The study was supported by the Natural Science Foundation of Hunan Province (2022JJ40252).

Disclosure of conflict of interest

None.

Address correspondence to: Zan Li, Hunan Cancer Hospital and The Affiliated Cancer Hospital of Xiangya School of Medicine, Central South University, Changsha 410008, Hunan, The People's Republic of China. Tel: +86-0731-89762250; E-mail: zzanli@163.com; Si-Qing Ma, Department of Pharmacy, Hunan Chest Hospital, Changsha 4100013, Hunan, The People's Republic of China. Tel: +86-0731-88867635; E-mail: maxiao5w@163.com

References

[1] Sung H, Ferlay J, Siegel RL, Laversanne M, Soerjomataram I, Jemal A and Bray F. Global cancer statistics 2020: GLOBOCAN estimates of incidence and mortality worldwide for 36 cancers in 185 countries. CA Cancer J Clin 2021; 71: 209-249.

[2] Siegel RL, Miller KD, Fuchs HE and Jemal A. Cancer statistics, 2022. CA Cancer J Clin 2022; 72: 7-33.

[3] Polyak K. Heterogeneity in breast cancer. J Clin Invest 2011; 121: 3786-3788.

[4] Linder MC and Hazegh-Azam M. Copper biochemistry and molecular biology. Am J Clin Nutr 1996; 63: 797S-811S.

[5] Jiang Y, Huo Z, Qi X, Zuo T and Wu Z. Copper-induced tumor cell death mechanisms and antitumor theragnostic applications of copper complexes. Nanomedicine (Lond) 2022; 17: 303-324.

[6] Tsvetkov P, Coy S, Petrova B, Dreishpoon M, Verma A, Abdusamad M, Rossen J, Joesch-Cohen L, Humeidi R, Spangler RD, Eaton JK, Frenkel E, Kocak M, Corsello SM, Lutsenko S, Kanarek N, Santagata S and Golub TR. Copper induces cell death by targeting lipoylated TCA cycle proteins. Science 2022; 375: 1254-1261.

[7] Gao W, Huang Z, Duan J, Nice EC, Lin J and Huang C. Elesclomol induces copper-dependent ferroptosis in colorectal cancer cells via degradation of ATP7A. Mol Oncol 2021; 15: 3527-3544.

[8] Kuo HW, Chen SF, Wu CC, Chen DR and Lee JH. Serum and tissue trace elements in patients with breast cancer in Taiwan. Biol Trace Elem Res 2002; 89: 1-11.

[9] Ding X, Jiang M, Jing H, Sheng W, Wang X, Han J and Wang L. Analysis of serum levels of 15 trace elements in breast cancer patients in Shandong, China. Environ Sci Pollut Res Int 2015; 22: 7930-7935.

[10] Ribeiro SM, Moya AM, Braga CB, Domenici FA, Feitosa MR, Feres O, Rocha JJ and Cunha SF. Copper-Zinc ratio and nutritional status in colorectal cancer patients during the perioperative period. Acta Cir Bras 2016; 31 Suppl 1: 24-28.

[11] Sohrabi M, Gholami A, Azar MH, Yaghoobi M, Shahi MM, Shirmardi S, Nikkhah M, Kohi Z, Salehpour D, Khoonsari MR, Hemmasi G, Zamani F, Sohrabi M and Ajdarkosh H. Trace element and heavy metal levels in colorectal cancer: comparison between cancerous and non-cancerous tissues. Biol Trace Elem Res 2018; 183: 1-8.

[12] Stepien M, Jenab M, Freisling H, Becker NP, Czuban M, Tjønneland A, Olsen A, Overvad K, Boutron-Ruault MC, Mancini FR, Savoye I, Katzke V, Kühn T, Boeing H, Iqbal K, Trichopoulou A, Bamia C, Orfanos P, Palli D, Sieri S, Tumino R, Naccarati A, Panico S, Bueno-de-Mes-

quita HBA, Peeters PH, Weiderpass E, Merino S, Jakszyn P, Sanchez MJ, Dorronsoro M, Huerta JM, Barricarte A, Boden S, van Guelpen B, Wareham N, Khaw KT, Bradbury KE, Cross AJ, Schomburg L and Hughes DJ. Pre-diagnostic copper and zinc biomarkers and colorectal cancer risk in the European Prospective Investigation into Cancer and Nutrition cohort. Carcinogenesis 2017; 38: 699-707.

[13] Oyama T, Matsuno K, Kawamoto T, Mitsudomi T, Shirakusa T and Kodama Y. Efficiency of serum copper/zinc ratio for differential diagnosis of patients with and without lung cancer. Biol Trace Elem Res 1994; 42: 115-127.

[14] Dìez M, Cerdàn FJ, Arroyo M and Balibrea J. Use of the copper/zinc ratio in the diagnosis of lung cancer. Cancer 1989; 63: 726-730.

[15] Baltaci AK, Dundar TK, Aksoy F and Mogulkoc R. Changes in the serum levels of trace elements before and after the operation in thyroid cancer patients. Biol Trace Elem Res 2017; 175: 57-64.

[16] Khanna SS and Karjodkar FR. Circulating immune complexes and trace elements (copper, iron and selenium) as markers in oral precancer and cancer: a randomised, controlled clinical trial. Head Face Med 2006; 2: 33.

[17] Basu S, Singh MK, Singh TB, Bhartiya SK, Singh SP and Shukla VK. Heavy and trace metals in carcinoma of the gallbladder. World J Surg 2013; 37: 2641-2646.

[18] Saleh SAK, Adly HM, Abdelkhaliq AA and Nassir AM. Serum levels of selenium, zinc, copper, manganese, and iron in prostate cancer patients. Curr Urol 2020; 14: 44-49.

[19] Schweigel-Röntgen M. The families of zinc (SLC30 and SLC39) and copper (SLC31) transporters. Curr Top Membr 2014; 73: 321-355.

[20] Brady DC, Crowe MS, Turski ML, Hobbs GA, Yao X, Chaikuad A, Knapp S, Xiao K, Campbell SL, Thiele DJ and Counter CM. Copper is required for oncogenic BRAF signalling and tumorigenesis. Nature 2014; 509: 492-496.

[21] Yu Z, Zhou R, Zhao Y, Pan Y, Liang H, Zhang JS, Tai S, Jin L and Teng CB. Blockage of SLC31A1-dependent copper absorption increases pancreatic cancer cell autophagy to resist cell death. Cell Prolif 2019; 52: e12568.

[22] Tsang T, Posimo JM, Gudiel AA, Cicchini M, Feldser DM and Brady DC. Copper is an essential regulator of the autophagic kinases ULK1/2 to drive lung adenocarcinoma. Nat Cell Biol 2020; 22: 412-424.

[23] Cobine PA and Brady DC. Cuproptosis: cellular and molecular mechanisms underlying copper-induced cell death. Mol Cell 2022; 82: 1786-1787.

[24] Ren X, Li Y, Zhou Y, Hu W, Yang C, Jing Q, Zhou C, Wang X, Hu J, Wang L, Yang J, Wang H, Xu H, Li H, Tong X, Wang Y and Du J. Overcoming the compensatory elevation of NRF2 renders hepatocellular carcinoma cells more vulnerable to disulfiram/copper-induced ferroptosis. Redox Biol 2021; 46: 102122.

[25] Feng C, Ma F, Hu C, Ma JA, Wang J, Zhang Y, Wu F, Hou T, Jiang S, Wang Y and Feng Y. SOX9/miR-130a/CTR1 axis modulates DDP-resistance of cervical cancer cell. Cell Cycle 2018; 17: 448-458.

[26] Shang X, Lin X, Manorek G and Howell SB. Claudin-3 and claudin-4 regulate sensitivity to cisplatin by controlling expression of the copper and cisplatin influx transporter CTR1. Mol Pharmacol 2013; 83: 85-94.

[27] Jiang P, Chen A, Wu X, Zhou M, Ul Haq I, Mariyam Z and Feng Q. NEAT1 acts as an inducer of cancer stem cell-like phenotypes in NSCLC by inhibiting EGCG-upregulated CTR1. J Cell Physiol 2018; 233: 4852-4863.

[28] Kuo MT, Fu S, Savaraj N and Chen HH. Role of the human high-affinity copper transporter in copper homeostasis regulation and cisplatin sensitivity in cancer chemotherapy. Cancer Res 2012; 72: 4616-4621.

[29] Chen HH, Song IS, Hossain A, Choi MK, Yamane Y, Liang ZD, Lu J, Wu LY, Siddik ZH, Klomp LW, Savaraj N and Kuo MT. Elevated glutathione levels confer cellular sensitization to cisplatin toxicity by up-regulation of copper transporter hCtr1. Mol Pharmacol 2008; 74: 697-704.

[30] Fu S, Naing A, Fu C, Kuo MT and Kurzrock R. Overcoming platinum resistance through the use of a copper-lowering agent. Mol Cancer Ther 2012; 11: 1221-1225.

[31] Baxevanis CN, Sofopoulos M, Fortis SP and Perez SA. The role of immune infiltrates as prognostic biomarkers in patients with breast cancer. Cancer Immunol Immunother 2019; 68: 1671-1680.

[32] Su Y, Zhang X, Li S, Xie W and Guo J. Emerging roles of the copper-CTR1 axis in tumorigenesis. Mol Cancer Res 2022; 20: 1339-1353.

[33] Voli F, Valli E, Lerra L, Kimpton K, Saletta F, Giorgi FM, Mercatelli D, Rouaen JRC, Shen S, Murray JE, Ahmed-Cox A, Cirillo G, Mayoh C, Beavis PA, Haber M, Trapani JA, Kavallaris M and Vittorio O. Intratumoral copper modulates PD-L1 expression and influences tumor immune evasion. Cancer Res 2020; 80: 4129-4144.

[34] Tang Z, Li C, Kang B, Gao G, Li C and Zhang Z. GEPIA: a web server for cancer and normal gene expression profiling and interactive analyses. Nucleic Acids Res 2017; 45: W98-W102.

[35] Chandrashekar DS, Karthikeyan SK, Korla PK, Patel H, Shovon AR, Athar M, Netto GJ, Qin ZS, Kumar S, Manne U, Creighton CJ and Varambal-

ly S. UALCAN: an update to the integrated cancer data analysis platform. Neoplasia 2022; 25: 18-27.
[36] Lánczky A and Győrffy B. Web-based survival analysis tool tailored for medical research (KMplot): development and implementation. J Med Internet Res 2021; 23: e27633.
[37] Li T, Fu J, Zeng Z, Cohen D, Li J, Chen Q, Li B and Liu XS. TIMER2.0 for analysis of tumor-infiltrating immune cells. Nucleic Acids Res 2020; 48: W509-W514.
[38] Ru B, Wong CN, Tong Y, Zhong JY, Zhong SSW, Wu WC, Chu KC, Wong CY, Lau CY, Chen I, Chan NW and Zhang J. TISIDB: an integrated repository portal for tumor-immune system interactions. Bioinformatics 2019; 35: 4200-4202.
[39] Li H, Wu N, Liu ZY, Chen YC, Cheng Q and Wang J. Development of a novel transcription factors-related prognostic signature for serous ovarian cancer. Sci Rep 2021; 11: 7207.
[40] Nazari SS and Mukherjee P. An overview of mammographic density and its association with breast cancer. Breast Cancer 2018; 25: 259-267.
[41] Ge EJ, Bush AI, Casini A, Cobine PA, Cross JR, DeNicola GM, Dou QP, Franz KJ, Gohil VM, Gupta S, Kaler SG, Lutsenko S, Mittal V, Petris MJ, Polishchuk R, Ralle M, Schilsky ML, Tonks NK, Vahdat LT, Van Aelst L, Xi D, Yuan P, Brady DC and Chang CJ. Connecting copper and cancer: from transition metal signalling to metalloplasia. Nat Rev Cancer 2022; 22: 102-113.
[42] Kahlson MA and Dixon SJ. Copper-induced cell death. Science 2022; 375: 1231-1232.
[43] Stanton SE and Disis ML. Clinical significance of tumor-infiltrating lymphocytes in breast cancer. J Immunother Cancer 2016; 4: 59.
[44] Gentles AJ, Newman AM, Liu CL, Bratman SV, Feng W, Kim D, Nair VS, Xu Y, Khuong A, Hoang CD, Diehn M, West RB, Plevritis SK and Alizadeh AA. The prognostic landscape of genes and infiltrating immune cells across human cancers. Nat Med 2015; 21: 938-945.
[45] Su Y, Zhang X, Li S, Xie W and Guo J. Emerging roles of the copper-CTR1 axis in tumorigenesis. Mol Cancer Res 2022; 20: 1339-1353.
[46] Munir MT, Kay MK, Kang MH, Rahman MM, Al-Harrasi A, Choudhury M, Moustaid-Moussa N, Hussain F and Rahman SM. Tumor-associated macrophages as multifaceted regulators of breast tumor growth. Int J Mol Sci 2021; 22: 6526.
[47] Cassetta L, Fragkogianni S, Sims AH, Swierczak A, Forrester LM, Zhang H, Soong DYH, Cotechini T, Anur P, Lin EY, Fidanza A, Lopez-Yrigoyen M, Millar MR, Urman A, Ai Z, Spellman PT, Hwang ES, Dixon JM, Wiechmann L, Cousens LM, Smith HO and Pollard JW. Human tumor-associated macrophage and monocyte transcriptional landscapes reveal cancer-specific reprogramming, biomarkers, and therapeutic targets. Cancer Cell 2019; 35: 588-602, e510.
[48] Choi J, Gyamfi J, Jang H and Koo JS. The role of tumor-associated macrophage in breast cancer biology. Histol Histopathol 2018; 33: 133-145.
[49] Sousa S, Brion R, Lintunen M, Kronqvist P, Sandholm J, Mönkkönen J, Kellokumpu-Lehtinen PL, Lauttia S, Tynninen O, Joensuu H, Heymann D and Määttä JA. Human breast cancer cells educate macrophages toward the M2 activation status. Breast Cancer Res 2015; 17: 101.
[50] Mao X, Xu J, Wang W, Liang C, Hua J, Liu J, Zhang B, Meng Q, Yu X and Shi S. Crosstalk between cancer-associated fibroblasts and immune cells in the tumor microenvironment: new findings and future perspectives. Mol Cancer 2021; 20: 131.
[51] Luo C, Wang P, He S, Zhu J, Shi Y and Wang J. Progress and prospect of immunotherapy for triple-negative breast cancer. Front Oncol 2022; 12: 919072.
[52] Schmid P, Adams S, Rugo HS, Schneeweiss A, Barrios CH, Iwata H, Diéras V, Hegg R, Im SA, Shaw Wright G, Henschel V, Molinero L, Chui SY, Funke R, Husain A, Winer EP, Loi S and Emens LA; IMpassion130 Trial Investigators. Atezolizumab and Nab-paclitaxel in advanced triple-negative breast cancer. N Engl J Med 2018; 379: 2108-2121.
[53] Liu H, Yang Z, Lu W, Chen Z, Chen L, Han S, Wu X, Cai T and Cai Y. Chemokines and chemokine receptors: a new strategy for breast cancer therapy. Cancer Med 2020; 9: 3786-3799.

Table S1. Correlation between SLC31A1 expression and clinicopathological parameters of BRCA

Clinicopathological characteristics	Low expression of SLC31A1 (n=541)	High expression of SLC31A1 (n=542)	*P* value
T stage n, (%)			0.610
T1	140 (13%)	137 (12.7%)	
T2	312 (28.9%)	317 (29.4%)	
T3	73 (6.8%)	66 (6.1%)	
T4	14 (1.3%)	21 (1.9%)	
N stage n, (%)			0.251
N0	266 (25%)	248 (23.3%)	
N1	179 (16.8%)	179 (16.8%)	
N2	60 (5.6%)	56 (5.3%)	
N3	30 (2.8%)	46 (4.3%)	
M stage n, (%)			0.616
M0	435 (47.2%)	467 (50.7%)	
M1	8 (0.9%)	12 (1.3%)	
Age, median (IQR)	58 (48, 67)	58 (49, 67)	0.930

Table S2. Correlation between SLC31A1 and gene markers of immune cells in TIMER 2.0 platform

CD8+ T cell	CD8A	0.113	0.000172	0.108	0.000628
	CD8B	0.038	0.213	0.033	0.102
T cell (general)	CD18	0.133	1.14E-06	0.132	8.87E-07
	CD3D	0.045	0.133	0.033	0.302
	CD3E	0.08	0.00762	0.073	0.0214
CD4+ T cell	CD4	0.203	1.18E-11	0.208	0.009098
	CD127	0.311	5.13E-26	0.341	2.05E-28
MDC	LYZ	0.275	1.60E-20	0.298	7.23E-22
	IRF7	-0.236	2.20E-15	-0.247	2.92E-15
TAM	CCL18	0.174	6.33E-09	0.196	4.43E-10
	CD163	0.305	4.26E-25	0.31	1.18E-23
	IL10	0.238	1.19E-15	0.24	1.65E-14
	CD206	0.269	9.59E-20	0.282	1.32E-19
M1 macrophage	NOS2	0.097	0.001335	0.094	0.003019
	IRF5	0.027	0.374	0.013	0.678
M2 macrophage	VSIG4	0.201	1.82E-11	0.195	5.81E-10
	MS4A4A	0.257	5.44E-18	0.264	2.36E-17
	CLEC7A	0.333	6.32E-30	0.337	7.86E-28
	CD273	0.306	2.78E-25	0.33	1.02E-26
Mast cell	CST3	-0.35	4.97E-33	-0.361	6.92E-32
	CPA3	0.104	0.000555	0.101	0.001432
Monocyte	CD86	0.244	2.45E-16	0.247	2.91E-15
	CD115	0.173	7.93E-09	0.163	2.30E-07
Neutrophils	CD66b	0.011	0.708	0.015	0.835
	CD11b	0.252	2.01E-17	0.237	4.13E-14
	CCR7	0.078	0.009258	0.077	0.015706
	FCGR3B	0.199	2.73E-11	0.208	3.70E-11
	CSF3R	0.026	0.396	0.008	0.886

Tregs	FOXP3	0.217	3.46E-13	0.226	6.07E-13
	CCR8	0.332	1.12E-29	0.334	2.63E-27
	STAT5B	0.102	0.000726	0.088	0.005358
	TGFB1	-0.018	0.759	-0.048	0.234
	CCR10	-0.16	1.04E-07	-0.175	2.88E-08
	CD25	0.277	8.88E-21	0.286	3.53E-20
	CD52	0.035	0.363	0.015	0.63
	CMTM7	-0.02	0.516	-0.035	0.384
Tfh	BCL6	0.131	0.001036	0.146	0.002355
	IL21	0	0.998	-0.012	0.711
	BATF	-0.238	1.41E-15	-0.251	8.46E-16
	CXCR5	0.047	0.117	0.035	0.276
Th1	TBX21	0.089	0.002998	0.084	0.007957
	STAT4	0.152	4.45E-07	0.15	2.04E-06
	STAT1	0.359	8.28E-35	0.351	3.33E-30
	IFNG	0.159	1.20E-07	0.162	3.06E-07
	TNF	0.095	0.001535	0.094	0.002871
Th2	GATA3	-0.113	0.000165	-0.131	3.62E-05
	STAT6	0.064	0.032748	0.063	0.047559
	STAT5A	0.03	0.314	0.009	0.773
	IL13	0.09	0.002724	0.087	0.00586
Th17	STAT3	0.367	1.99E-36	0.349	8.01E-30
	IL17A	0.099	0.001022	0.097	0.002136
B cell	CD19	-0.007	0.818	-0.031	0.322
	CD79A	0.014	0.632	0	1
	CD79B	-0.063	0.035403	-0.103	0.001184
	MS4A1	0.055	0.067	0.044	0.167
T cell exhaustion	PDCD1	0.02	0.502	0.003	0.918
	PDCD1LG2	0.306	2.78E-25	0.33	1.02E-26
	CTLA4	0.142	2.28E-06	0.14	8.91E-06
	LAG3	0.032	0.295	0.025	0.424
	HAVCR2	0.265	4.17E-19	0.265	1.98E-17
	GZMB	0.099	0.0009802	0.094	0.002890752

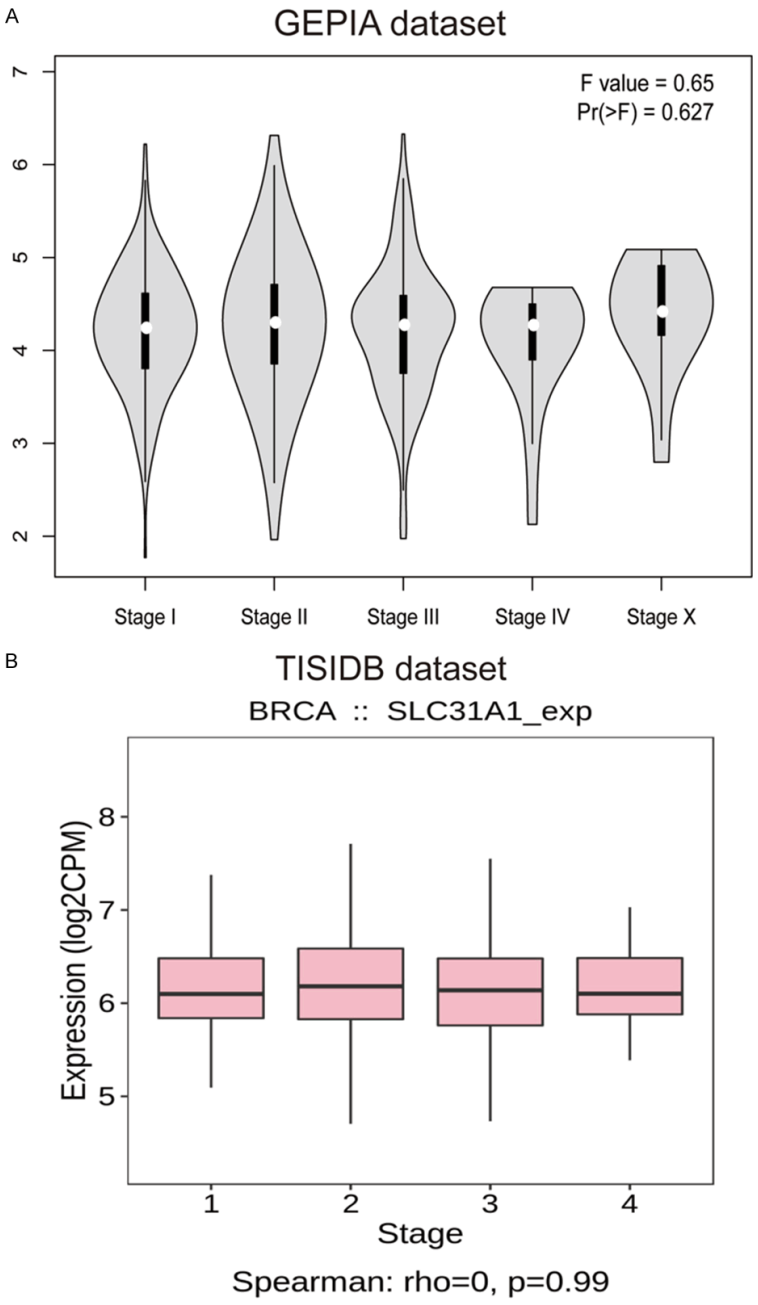

Figure S1. Correlation between SLC31A1 mRNA expression and cancer stage in GEPIA dataset (A) and TISIDB dataset (B).

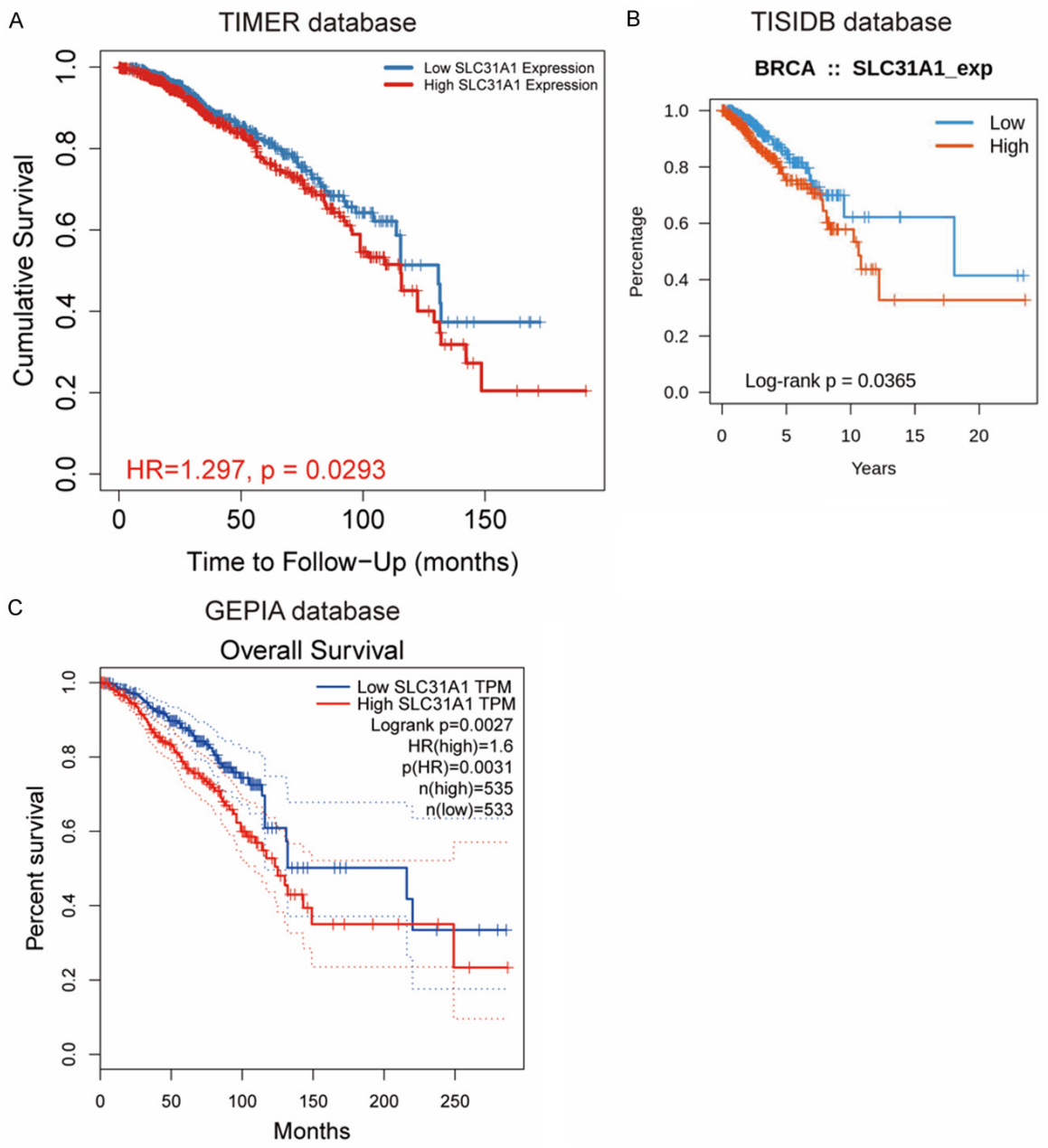

Figure S2. The association between SLC31A1 expression and OS in BRCA in TIMER dataset (A), TISIDB dataset (B) and GEPIA dataset (C).

Table S3. Correlation between SLC31A1 and gene markers of TAM, M1 macrophage, M2 macrophage, Neutrophils, Tregs, Th1, Th2, Th17 and T cell exhaustion in GEPIA dataset

Description	Gene markers	BRCA			
		BRCA tissues		Normal tissues	
		Rho	*p* value	Rho	*p* value
TAM	CCL18	0.13	**	0.0069	0.94
	CD206	0.05	0.1	-0.17	0.07
	CD163	0.17	***	-0.17	0.074
	IL10	0.21	***	-0.17	0.067
M1 macrophage	NOS2	0.022	0.65	0.11	0.26
	IRF5	0.13	*	0.15	0.1
M2 macrophage	VSIG4	0.15	***	-0.17	0.067
	MS4A4A	0.24	***	-0.19	*
	CLEC7A	0.20	***	0.38	***
	CD273	0.28	***	-0.036	0.71
Neutrophils	CD66b	-0.012	0.69	-0.058	0.54
	CD11b	0.16	***	-0.052	0.58
	CCR7	-0.0032	0.92	0.099	0.30
	FCGR3B	0.0017	0.57	-0.1	0.29
	CSF3R	0.00063	0.98	0.35	***
Tregs	FOXP3	0.12	***	0.31	***
	CCR8	0.25	***	0.062	0.52
	STAT5B	0.102	***	0.11	0.25
	TGFB1	-0.018	0.759	-0.048	0.234
	CCR10	-0.16	***	-0.175	***
	CD25	0.277	***	0.286	***
	CD52	0.035	0.363	0.015	0.630
	CMTM7	-0.02	0.516	-0.035	0.384
Th1	TBX21	0.089	**	0.084	**
	STAT4	0.047	0.12	0.150	***
	STAT1	0.28	***	0.28	**
	IFNG	0.16	***	0.0084	0.93
	TNF	0.07	*	-0.032	0.74
Th2	GATA3	-0.13	***	0.6	***
	STAT6	0.087	**	0.55	***
	STAT5A	0.05	0.098	-0.34	***
	IL13	0.085	**	0.0053	0.96
Th17	STAT3	0.3	***	0.73	***
	IL17A	0.016	0.59	0.046	0.63
T cell exhaustion	PDCD1	0.019	0.53	0.11	0.25
	PDCD1LG2	0.28	***	-0.036	0.71
	CTLA4	0.11	***	0.13	0.18
	LAG3	0.083	**	0.17	0.079
	HAVCR2	0.27	***	-0.048	0.62
	GZMB	0.11	***	-0.15	0.12

Note: TAM: Tumor-associated macrophage; Tregs: Regulatory T cell; BRCA: Breast cancer; *$P < 0.01$; **$P < 0.001$; ***$P < 0.0001$.